Oct 18th

A Design Procedure for Lipped Channel Flexural Members

Maria E. Moreyra

Teoman Pekoz

Twelfth International Specialty Conference on Cold-Formed Steel Structures
St. Louis, Missouri, U.S.A., October 18-19, 1994

A DESIGN PROCEDURE FOR LIPPED CHANNEL FLEXURAL MEMBERS

Maria E. Moreyra[1] and Teoman Peköz[2]

ABSTRACT

This paper is third in a series of three papers describing the research sponsored by the American Iron and Steel Institute. Physical test results described in the first paper combined with the finite element solution parametric studies described in the second paper were used in this paper to develop improved design procedures for edge stiffened elements.

1. INTRODUCTION

Test results [Willis and Wallace (1990a and b)] on lipped channel flexural members have shown some disagreement with the values predicted by the AISI Specification (1991). The main reason for the discrepancies is thought to be the provisions for edge stiffened compression elements. This paper is third in a series of three papers describing the research sponsored at Cornell University by the American Iron and Steel Institute to develop improved design procedures for edge stiffened elements.

This study involves looking at the interaction of different plate elements such as web, flange and lip of a lipped channel section. A design procedure is proposed and the results of this procedure are compared to those obtained from physical tests reported by Moreyra and Peköz (1994a) and to finite element solution (ABAQUS) results reported by Moreyra and Peköz (1994a)

2 EFFECTIVE WEB DESIGN

Several design procedures have been proposed in the past to improve the design equations for web elements. The behavior of the edge stiffened element depends not only on the edge stiffener but also on the web. In this section, various web design procedures are evaluated on the basis of experimental and analytical results.

2.1 AISI SPECIFICATION (1991) PROCEDURE

Effective areas for webs given in the AISI Specification (1991) are illustrated in Fig. 1. The calculation of the effective widths b_1 and b_2 involves the buckling coefficient, k calculated as follows:

$$k = 4 + 2(1-\psi)^3 + 2(1-\psi) \tag{2.1}$$

where
$\psi = f_2/f_1$ (compression = +, tension = -)

The effective widths, b_1 and b_2 shown in Fig. 2, are calculated as

$$b_1 = \frac{b_e}{3-\psi} \tag{2.2}$$

$$b_2 = \begin{cases} \dfrac{b_e}{2} & \text{if } \psi \le -0.236 \\ b_e - b_1 & \text{if } \psi > -0.236 \end{cases} \tag{2.3}$$

where b_e is the effective width of the web element calculated as follows:

---

[1] Engineer, L. E. Robertson Assoc., N. Y., N. Y.

[2] Professor of Structural Engineering, Cornell University, Ithaca, N.Y.

$$b_e = \rho h \tag{2.4}$$

$$\rho = (1-0.22/\lambda) \; / \; \lambda \tag{2.5}$$

$$\lambda = \frac{1.052}{\sqrt{k}} \left(\frac{h}{t}\right) \sqrt{\frac{f}{E}} \tag{2.6}$$

and $f = f_1$.

2.2 EUROCODE PROCEDURE

The Eurocode 3 (1992) method also uses the effective width model of Fig. 1. Values of b_1 , b_2 and k differ from those of the AISI Specification (1991):

$$b_1 = 0.4\rho b_c \tag{2.7}$$

$$b_2 = 0.6\rho b_c \tag{2.8}$$

$$k = 7.81 - 6.29\psi + 9.78\psi^2 \qquad (for\ \psi < 0) \tag{2.9}$$

The variable b_c is the width of the compression portion of the web, ρ is given by Eq. 2.5, and ψ is the ratio of tension stress (a negative value) to compression stress (a positive value). Even though ρ is multiplied by b_c, ρ is based on the full web flat width. These equations are substituted into the AISI Specification to examine their accuracy. Correlations to test results are summarized in Table 1. It is clear that the Eurocode web equation most precisely predicts the bending capacity of the ABAQUS and Experimental specimens.

2.3 SOOI (1993) APPROACH

Sooi (1993) proposes a different effective width model. The effective stresses are assumed to be distributed as shown in Fig. 1. The total effective web width b_e is calculated using the AISI Specification which uses Eq. 2.1 to calculate k. Instead of separating the effective compressive stresses into b_1 and b_2 (as seen in Fig. 1), it is assumed that all the compressive stresses in the web to be located at the flange-web intersection (as seen in Fig. 2). Therefore, he proposes

$$b_1 = b_e - b_t \tag{2.10}$$

where b_t is the tension portion of the web shown in Fig. 1. Its correlation with the test results is examined in Table 1. This approach has a relatively high coefficient of variation when compared to the ABAQUS test results. Correlations to experimental test results are very good.

3 MAXIMUM EDGE STRESS

The finite element analyses show that the maximum stresses in the section oftentimes do not reach yield. The AISI Specification design procedure, however, assumes that edge stresses, f, equal yield, F_y. The authors recommend that f equal a nominal stress, F_n, in the AISI design procedure. In other words, it is suggested that F_n be applied in the following calculations: λ for the flange, web, and lip (see Eq. 2.6), and in the nominal moment capacity

calculation, $M_n = F_n S_e$ where S_e equals the section modulus of the effective section.

A nominal edge stress assumption proposed by Bernard, Bridge, and Hancock (1993) yields good correlations to tests. Their proposed equation however, requires the calculation of the distortional buckling stress of the section, σ_{de}. This value is not easily obtained. Therefore, the authors developed an empirical equation for F_n which avoids calculation of the distortional buckling stress, σ_{de}. It yields F_n values close to those calculated by Bernard, Bridge, and Hancock (1993) and takes into account the ABAQUS flange stresses. The empirically developed equation which best correlates to the test results is:

$$F_n = \frac{F_y}{\left(\frac{h}{t}\right)^{2/3}\left(0.186 + 0.114\frac{w}{h}\right)^2} \leq F_y \qquad (3.1)$$

where h, w, and T are the web flat height, flange flat width, and the section thickness.

Stresses obtained using Eq. 3.1 are compared with the ABAQUS flange stresses in Fig. 3. Details of the ABAQUS stresses plotted in Fig. 3 are described in Moreyra and Pekoz (1994b). Since distortional buckling involves larger deformations at the lip/flange edge than local buckling, it is quite possible that these ABAQUS stresses are not representative of a nominal edge stress. The plots in Fig. 3 distinguish between the failure modes (local or distortional) of each section.

The relationship between the flange, the web, and the ABAQUS flange stress for local buckling failures is fairly accurately predicted by Eq. 3.1. It would appear that F_n values are too high compared to ABAQUS. The ABAQUS stresses plotted are probably slightly lower than the actual flange stresses at failure. This is because the stresses recorded were one ABAQUS load increment before failure.

Values of F_n from Eq. 3.1 are plotted in Fig. 4 as a function of w/h. It can be seen that the largest difference between F_n and F_y is for the larger w/h ratios. This curve resembles the effective width ratio curve.

The value for F_n was substituted for f in the AISI Specification to make strength predictions of all tests described in this study. Results are shown in Table 2. The correlations with ABAQUS and experimental test results improve by 15% and 7%, respectively. The COV of the M_t/M_n also improves significantly.

4 EDGE-STIFFENED FLANGE DESIGN

The current AISI design procedure for uniformly compressed edge stiffened elements depends on the flange buckling coefficient, k, and the adequate stiffener moment of inertia, I_a. Both variables depend on which "Case" the element belongs to: the elastic buckling case or the post-buckling case. The final design, therefore, is very "Case" dependent.

4.1 ADEQUATE EDGE STIFFENER

An edge stiffener (lip) is "adequate" when its length is sufficient to cause the flange to buckle in the local mode, yet short enough to prevent the lip from buckling itself. In other words, when the local buckling stress equals the distortional buckling stress ($\sigma_k = \sigma_{de}$), one has found the adequate lip size.

Desmond (1978) developed the adequate stiffener size requirements presently used in the AISI Specification. He assumed a web height equal to the flange width when deriving these equations. Since sophisticated programs were not

available during the time of his research, he used linear stability equations to predict the elastic buckling behavior of edge stiffened elements. The equations for the post-buckling case were developed empirically based on test results. These tests, however, were set up so that the web behavior would not influence the flange. Therefore, the edge-stiffened design equations in the AISI Specification assume that the web does not influence the flange.

An elastic buckling finite-strip analysis using the BFINST [Hancock (1978)] was carried out on the parametric study sections to determine the adequate stiffener size. Two observations were very clear: I_a is a function of flange width *and* web height, and the AISI curve inaccurately defines the adequate lip size for a variety of web heights. If web buckling controls, the adequate stiffener size increases with increasing plate slenderness; vice versa if flange buckling controls.

Formulating design equations for an edge stiffened compression element based on I_a, as done in the AISI Specification, appears to be rather complicated. This parameter depends on many variables which are difficult to incorporate in a simple design equation. Even if I_a is determined, an accurate value for k still must be derived. The ultimate goal is to arrive at a value for λ, the buckling slenderness ratio for the flange. The authors feel that it is more efficient and more accurate to directly develop design formulas for λ. This value should be a function of lip size *and* web height since both elements provide a support or boundary condition to the flange. If lip size increases, while all other dimensions remain the same, λ should reach an optimum value, the local buckling value. Beyond this optimum value, λ should remain constant with increasing lip size.

4.2 SHARP'S APPROACH TO λ

Sharp (1966, 1993) gives an approximate solution of the compressive strength of flanges with a stiffening lip. The compression flange and lip is analyzed as "column" undergoing torsional buckling about the web-flange intersection. The lipped flange is assumed to be restrained against rotation at the attached edge by the other elements of the section. A cross-section of the "column" model is shown in Fig. 5.

The buckling strengths of plates and columns may be represented by

$$F_{cr} = \frac{\pi^2 E}{\lambda_e^2} \tag{4.1}$$

where F_{cr} = buckling stress, E = modulus of elasticity, and λ_e = equivalent slenderness ratio.

If the flange undergoes local buckling, Eq. 4.1 may be substituted into the plate buckling equation

$$F_{cr} = \frac{k\pi^2 E}{12(1-\nu^2)(w/t)^2} \tag{4.2}$$

using k = 4.0 and the following equivalent slenderness ratio for local buckling, λ_{el}, is obtained:

$$\lambda_{el} = \left(\frac{w}{t}\right)\sqrt{\frac{12(1-\nu^2)}{k}} = 1.65\left(\frac{w}{t}\right) \tag{4.3}$$

Sharp (1993) derives the following distortional buckling equivalent slenderness ratio, λ_{ed} , assuming the "column" buckles about a fixed axis of rotation (the flange-web intersection):

$$\lambda_{ed} = \pi \sqrt{\frac{I_p}{0.375\, J + 2\sqrt{\frac{K_\phi C_w}{E}}}} \tag{4.4}$$

where

$I_p = I_{xo} + I_{yo}$ = polar moment of inertia of lip and flange about center of rotation.

I_{xo} , I_{yo} = moments of inertia of lip and flange about the horizontal and vertical axes at the center of rotation.

J = torsional constant of flange and lip .

C_w = the warping constant for lipped flange about center of rotation and is given by

$$C_w = \Gamma + w^2 \left(I_{yc} - \frac{wt^3}{12} \right) \tag{4.5}$$

Γ = the warping constant of combined lip and flange about the intersection of the stiffener and flange centerlines. For large lips, Γ is generally insignificant when compared to the second term and may be neglected. Note: If Γ is assumed zero, C_w becomes negative when $I_{yc} \leq wt^3/12$. The warping constant cannot be a negative number. Conservatively assuming a zero radius, d/t must be $\geq \frac{\sqrt{w/d}}{2}$ so that $C_w > 0$.

I_{yc} = moment of inertia of combined lip and flange about the centroidal axis parallel to the flange.

K_I = the rotational restraint offered to the flange by other elements of the section. Sharp modifies this variable to account for flange flexibility and defines it as

$$K_\phi = \frac{2\, D_w}{h} \left(\frac{1}{1 + \frac{2}{3} \frac{D_w}{D_p} \frac{w}{h}} \right) \tag{4.6}$$

D_p, D_w = the plate rigidities of the flange and web, respectively. If the thicknesses of the elements are the same, D_p and D_w are equal and defined as

$$D_w = D_p = \frac{Et^3}{12(1-\nu^2)} \tag{4.7}$$

h, w = flat widths of the web and flange elements, respectively.

Using the variables defined in Fig. 5, assuming a simple straight lip, and assuming equal element thicknesses, the previously described variables are:

$$u = 1.57r \tag{4.8}$$

$$c = 0.637r \tag{4.9}$$

$$I_{xo} = t\,[\,u(r-c)^2 + d(r + d/2)^2 + d^3/12] \tag{4.10}$$

$$I_{yo} = t\,[w^3/3 + u(w+c)^2 + d(w+r)^2] \tag{4.11}$$

$$J = \frac{t^3}{3}\,[w + u + d] \tag{4.12}$$

$$\bar{x} = \frac{u(r-c) + d(d/2 + r)}{w + u + d} \tag{4.13}$$

$$I_{yc} = t\,[w\bar{x}^2 + u(\bar{x} - r + c)^2 + d(d/2 + r - \bar{x})^2 + d^3/12] \tag{4.14}$$

One can substitute the column buckling F_{cr} (Eq. 4.3) into the buckling slenderness ratio, $\lambda = \sqrt{F_y/F_{cr}}$, to obtain:

$$\lambda = \sqrt{\frac{F_y}{F_{cr}}} = \sqrt{\frac{F_y}{\frac{\pi^2 E}{\lambda_e^2}}} = \frac{\lambda_e}{\pi}\sqrt{\frac{F_y}{E}} \tag{4.15}$$

$$\lambda_e = \lambda_{ed} \geq \lambda_{el} \tag{4.16}$$

If a nominal edge stress is assumed, it may be accurate to consider λ as a function of F_n:

$$\lambda = \frac{\lambda_e}{\pi}\sqrt{\frac{F_n}{E}} \tag{4.17}$$

$$\lambda_e = \lambda_{ed} \geq \lambda_{el} \tag{4.18}$$

The equivalent slenderness ratio used in λ equals the controlling of the two equivalent slenderness ratios. Implied in these equations is that once the distortional slenderness ratio equals the local slenderness ratio, an adequate lip size has been obtained. Local buckling then controls the section.

This λ was used in the AISI design procedure to predict the ultimate moments of ABAQUS models, and the experiments by all researchers discussed in Moreyra and Peköz (1994a). The results are summarized in Table 3. The following observations are made: The assumption $f = F_y$ correlates poorly to test results. λ as a function of F_n is slightly more unconservative than λ as a function of F_y. The COVs however, are lower when using F_n.

The results using Eq. 4.4 may be validated by comparing them with the minimum critical buckling stresses obtained by an elastic finite-strip buckling analysis program called BFINST [Hancock(1978)]. The λ_e in Eq. 4.1 must equal the larger of λ_{el} and λ_{ed} defined in Eqns. 4.3 and 4.4, respectively. Since Eq. 4.4 is for an edge-stiffened flange, the BFINST critical stresses can only be compared for those sections which undergo local flange buckling or distortional buckling. The BFINST values for sections that undergo local *web* buckling may not be included in this comparison. The BFINST minimum critical stresses and critical stresses from Eq. 4.1 are compared in Table 4. This table shows that the correlation is very good.

4.3 EUROCODE DESIGN METHOD

The Eurocode 3 (1992) method for determining the effective width of an edge stiffened flange element is an iterative procedure. It is based on the assumption that the stiffener works as a beam on an elastic foundation. The elastic foundation is represented by a spring stiffness which is a function of the bending stiffness of adjacent elements.

The assumed effective portions of an edge stiffened element is similar to that of the AISI Specification (1991). Eurocode further reduces the effective flange area by reducing the thickness of some portions of this element.

This method for determining the effective flange and lip area was applied using discussed web equations and two edge stresses, F_n and F_y. The correlations with the ABAQUS and experimental results is shown in Table 5. This table shows that when F_n is used in the design equations, the Eurocode method is conservative and has very high COVs. If F_y is applied to the design process, this method is unconservative when compared to the ABAQUS tests. The disadvantage of this method is the iterative procedure it entails. One may not be able to obtain a quick calculation without the aid of a computer.

5 CONCLUSIONS

The greatest improvement in the AISI Specification results when the edge stress, f, is set equal to a nominal edge stress, F_n. ABAQUS results show that stresses in the flange do not reach yield in many sections. Therefore, the AISI design process which assumes $f = F_y$ is not accurate according to ABAQUS. For these reasons, the authors suggest using $f = F_n$ in the AISI design provisions. The F_n value should be used in the λ equations for lip,

flange, and web, and in the nominal moment calculation, $M_n = F_n * S_e$, where S_e equals the section modulus of the effective section.

The existing AISI design procedure for determining the effective flange area can be improved. This is shown in the tables of this paper by comparing M_t / M_n ratios and coefficient of variations (COVs) of the AISI effective flange design methods to those of Eurocode or Sharp (assuming $f = F_n$). The authors have also shown that the effective flange area is clearly dependent on the web height. However, the AISI design equations assume that the web does not influence the flange behavior. The existing AISI design procedure of an edge stiffened element is quite complex and depends on many variables. The authors suggest applying a more accurate, and more direct design method for predicting the effective flange area.

If one assumes $f = F_y$ in the design process, the Eurocode method for determining an effective flange area is very unconservative. If one assumes $f = F_n$, strength predictions become very conservative. The disadvantage of the Eurocode process is the required iterative process which makes this method complex and inefficient.

Ultimately, one must arrive at a value for the flange buckling slenderness ratio, λ, in order to calculate the effective flange width. This value is defined as the square root of the post-buckling ultimate stress over F_{cr} (the critical buckling stress). Ever since Von Karman developed this equation in 1932, it was assumed that elements reach a stress equal to F_y at failure. Therefore, f in Eq. 2.6 is taken as F_y. If one uses F_n to calculate M_n directly, it would be more consistent and rational to assume $f = F_n$ in Eq. 2.6. However, predictions assuming λ as a function of F_n are slightly less conservative than λ as a function of F_y.

The F_{cr} values obtained using Eq. 4.1 compare well with F_{cr} values obtained by BFINST. Sharp approach is straight forward and correlates well to ABAQUS and experimental tests. Coefficients of variation for this approach are the lowest of all approaches applied. Since Sharp's method for determining the flange λ is direct, simple, accurate, theoretically based, a function of web height, and it correlates well to test results with a low coefficient of variation, the authors recommend Sharp approach to determine the effective area of an edge stiffened compression flange. The author also suggests making the λ equation a function of F_n in order to provide consistency in the design code.

Comparing all web design procedures to test results, the Eurocode method of determining the effective web area is the most conservative. The AISI method is the least conservative. The Eurocode and Sooi approaches reach approximately the same level of accuracy in its predictions. This is concluded since the difference in the average M_t / M_n ratio is always less than 3 percent. The COVs are approximately the same for all web equations. The simplest of all proposed procedures for web design is Sooi's method. For this reason, the authors suggest it as a modification to the AISI Specification.

Ultimate strength predictions using this suggested design procedure $M_{n\,S}$ are compared to AISI ultimate strength predictions $M_{n\,AISI}$ for each ABAQUS test result in Table 6, and for each experimental test result in Table 7. The $\frac{M_{n\,S}}{M_{n\,AISI}}$ ratio listed in these tables indicate the impact of the proposed provisions on the calculated capacities.

It is seen that the calculated capacities according to the proposed provisions are, on average, 11%, 18%, and 25% lower than those according to the AISI provisions for the 6", 8", and 10" deep web sections in the ABAQUS analyses, respectively. For the experimental sections, strength predictions according to the proposed provisions are an average of 15% lower than predictions made

by the AISI Specification. While these reductions may seem quite large, they are necessary to reduce the unconservative predictions inherent in the present specification.

6 ACKNOWLEDGEMENTS

This paper is based on a thesis presented to the Graduate School of Cornell University for the degree of Master of Science by Maria E. Moreyra. This work was sponsored at Cornell University by the American Iron and Steel Institute. The valuable support and contributions of the members of the AISI Subcommittee on Element Behavior and its Chairman Mr. D. L. Johnson are gratefully acknowledged.

APPENDIX - REFERENCES

ABAQUS (1989). Users Manual Version 4.8. Hibbit, Karlsson and Sorensen, Inc.

American Iron and Steel Institute (1991), " Load and Resistance Factor Design Specification for Cold-Formed Steel Structural Members, March 16, 1991 Edition

Bernard E. S., Bridge R. Q. and Hancock, G. J. (1993) "Intermediate Stiffeners in Cold-formed Profiled Steel Decks. Part I - "V" Shaped Stiffeners," Research Report R6J3, School of Civil and Mining Engineering, University of Sydney, Australia, 1993

Desmond, T. P., Peköz, T. and Winter, G. (1978), "Edge Stiffeners for Thin-Walled Members," Journal of the Structural Division, ASCE, Vol. 107, No. ST2

EUROCODE 3 (1992), "Design of Steel Structures, Part 1.3: Cold-Formed Thin Gauge Members and Sheeting," August 1992
Hancock, G. J.(1978), "BFINST6: An Elastic Finite Strip Buckling Analysis Program," University of Sydney, Australia, 1978

Moreyra, M. E. and Peköz, T. (1994a), "Experiments on Lipped Channel Flexural Members," Proceedings of the Twelfth International Specialty Conference on Cold-Formed Steel Structures, University of Missouri-Rolla, October 1994

Moreyra, M. E. and Peköz, T. (1994b), "Finite Element Studies on Lipped Channel Flexural Members," Proceedings of the Twelfth International Specialty Conference on Cold-Formed Steel Structures, University of Missouri-Rolla, October 1994

Schuster, R. (1992), "Testing of Perforated C-Stud Sections in Bending." University of Waterloo, Ontario. Paper for Canadian Sheet Steel Building Institute, March 1992

Sharp, M. L. (1966), "Longitudinal Stiffeners for Compression Members," Journal of the structural Division, ASCE ST5, Oct. 1966

Sharp, M. L. (1993), "Behavior and Design of Aluminum Structures," McGraw-Hill Inc., NY, 1993

Sooi, T. K. and Pekoz, T., Project Director (1993), "The Behavior of Component Elements of Aluminum Members," Research Report 93-1, School of Civil and Environmental Engineering, Cornell University, 1993

Willis, C. T. and Wallace, B. J.(1990a), "Behavior of Cold-Formed Steel Purlins Under Gravity Loading," Journal of Structural Engineering, Vol. 116, No. 8, August 1990, 2061-2069

Willis, C. T. and Wallace, B. J.(1990b), "Wide Lips - A Problem With the AISI Code," Proceeding of the Tenth International Specialty Conference on Cold-Formed Steel Structures, St. Louis, MO, October 23-24

APPENDIX - NOTATION

c, d, R, r, u, w, $\bar{x}$ Cross-sectional dimensions defined in Fig. 5
b_1, b_2, b_t Effective widths shown in Figs. 1 and 2
f_1, f_2 Stresses shown in Figs. 1 and 2
k Plate buckling coefficient
$M_{n\,S}$ Ultimate moment obtained using the design procedure suggested in the paper
$M_{n\,AISI}$ Ultimate moment obtained using the AISI Specification (1991)
ψ f_1/f_2
Several additional terms are defined in the paper

Table 1 Predictions of ABAQUS and experimental ultimate moments using various proposed web equations.

AISI MODIFICATION: Web Equation	ABAQUS tests		Experiments from Table 7 of Moreyra and Peköz (1994a)	
	AVG	COV(%)	AVG	COV(%)
AISI	0.805	8.53	0.859	8.94
EUROCODE	0.864	8.32	0.954	8.28
SOOI	0.856	9.28	0.942	6.56

AVG = average M_t / M_n of all tests
COV = M_t / M_n coefficient of variation
M_t from all experiments and ABAQUS
M_n = Predicted moment capacity

Table 2 Predictions of ABAQUS and experimental ultimate moments using various proposed web equations and f = F_n

AISI MODIFICATIONS:		ABAQUS tests		Experiments from Table 7 of Moreyra and Peköz (1994a)	
Edge Stress	Web Equation	AVG	COV(%)	AVG	COV(%)
f = F_n	AISI	0.950	5.73	0.926	7.50
	EUROCODE	1.024	6.91	1.027	6.37
	SOOI	0.999	6.76	1.001	6.20

AVG = average M_t / M_n of all tests
COV = M_t / M_n coefficient of variation
M_t from all experiments and ABAQUS
M_n = Predicted moment capacity

Table 3 Predictions of ABAQUS and experimental ultimate moments using the Sharp approach.

AISI MODIFICATION:			ABAQUS tests		Experiments from Table 7 of Moreyra and Peköz (1994a)	
Effective Flange	Edge Stress	Web Equation	AVG	COV(%)	AVG	COV(%)
λ = SHARP Eq. (4.9) [λ = funct. of F_y]	f = F_y	AISI	0.789	8.38	0.881	7.87
		EURO	0.848	8.44	0.977	7.67
		SOOI	0.840	9.48	0.964	7.11
	f = F_n	AISI	0.975	6.99	0.957	6.82
		EURO	1.050	8.03	1.063	6.74
		SOOI	1.023	7.94	1.035	7.02
λ = SHARP Eq. (4.10) [λ = funct. of F_n]	f = F_y	AISI	0.756	11.13	0.868	8.24
		EURO	0.812	11.16	0.962	7.91
		SOOI	0.808	11.65	0.949	7.07
	f = F_n	AISI	0.932	5.36	0.942	6.83
		EURO	1.005	5.57	1.046	6.45
		SOOI	0.982	6.75	1.019	6.64

AVG = average M_t / M_n of all tests
COV = M_t / M_n coefficient of variation

M_t from allexperiments and ABAQUS
M_n = Predicted moment capacity

Table 4 Comparison of BFINST minimum flange buckling stresses to Sharp F_{cr}. Stresses are in ksi units. 1 ksi = 6.895 N/mm^2

TEST	F_{cr} (BFINST)	F_{cr} (Sharp)	TEST	F_{cr} (BFINST)	F_{cr} (Sharp)
H1-W1-0.35	36	28.3	H2-W2-0.6	27	24.1
H1-W1-0.6	54	49.0	H2-W2-0.85	38	33.5
H1-W1-0.85	71	64.9	H2-W2-1.1	42	41.7
H1-W1-1.1	84	77.2	H2-W2-1.2	42	43.2
H1-W1-1.2	85	81.3	H2-W2-1.3	42	43.2
H1-W1-1.3	80	84.9	H2-W2-1.4	42	43.2
H1-W1-1.4	76	88.1			
H1-W2-0.6	31	26.7	H2-W3-0.6	17	14.5
H1-W2-0.85	43	37.4	H2-W3-0.85	25	21.6
H1-W2-1.0	48	43.1	H2-W3-1.0	27	24.2
H1-W2-1.1	48	43.2	H2-W3-1.1	27	24.2
H1-W2-1.2	48	43.2	H2-W3-1.2	27	24.2
H1-W3-0.6	20	16.5	H3-W3-0.6	16	13.8
H1-W3-0.85	27	23.9	H3-W3-0.85	23	19.9
H1-W3-1.0	27	24.2	H3-W3-0.95	25	22.2
H1-W3-1.1	27	24.2	H3-W3-1.0	25	23.3
H1-W3-1.2	27	24.2	H3-W3-1.1	25	24.2
H1-W3-1.3	27	24.2	H3-W3-1.2	25	24.2

Table 5 Predictions of ABAQUS and experimental ultimate moments using the Eurocode 3 method of determining effective compression flange area.

AISI MODIFICATION:			ABAQUS tests		Experiments from Table 7 of Moreyra and Peköz (1994a)	
Effective Flange	Edge Stress	Web Equation	AVG	COV(%)	AVG	COV(%)
EUROCODE 3	$f = F_y$	AISI	0.835	5.33	0.918	9.68
		EURO	0.897	4.85	1.025	9.19
		SOOI	0.885	6.09	1.007	7.25
	$f = F_n$	AISI	1.042	10.88	1.016	8.77
		EURO	1.126	11.25	1.137	8.00
		SOOI	1.090	10.47	1.100	7.56

AVG = average M_t / M_n of all tests

COV = M_t / M_n coefficient of variation

M_t from all experiments and ABAQUS

M_n = Predicted moment capacity

Table 6 Comparison of the AISI Predictions with the Suggested Design Procedure Pedictions of ABAQUS Results.

M_t = Ultimate moment calculated by ABAQUS (1989), k-in (1 k-in = 113 N-m)

TEST	M_t	$\frac{M_t}{M_{n\,AISI}}$	$\frac{M_t}{M_{n\,S}}$	$\frac{M_{n\,S}}{M_{n\,AISI}}$
H1-W0-0.6	44.0	0.884	0.896	0.987
H1-W0-0.8	46.2	0.883	0.886	0.997
H1-W0-1.1	47.9	0.906	0.902	1.005
H1-W1-0.3	39.2	0.808	0.816	0.990
H1-W1-0.6	48.7	0.877	0.920	0.953
H1-W1-0.8	54.7	0.887	0.927	0.956
H1-W1-1.1	59.3	0.927	0.937	0.989
H1-W1-1.2	60.5	0.956	0.947	1.009
H1-W1-1.3	61.7	0.988	0.959	1.030
H1-W1-1.4	62.5	1.017	0.966	1.052
H1-W2-0.6	47.2	0.793	0.915	0.867
H1-W2-0.8	55.7	0.833	0.971	0.858
H1-W2-1.0	57.4	0.803	0.928	0.865
H1-W2-1.1	59.5	0.816	0.952	0.857
H1-W2-1.2	59.5	0.822	0.950	0.865
H1-W3-0.6	42.4	0.690	0.868	0.795
H1-W3-0.8	50.4	0.729	0.924	0.789
H1-W3-1.0	53.3	0.716	0.933	0.768
H1-W3-1.1	55.5	0.714	0.949	0.753
H1-W3-1.2	56.5	0.721	0.963	0.749
H1-W3-1.3	58.1	0.745	0.988	0.754
H1-W0-0.6	60.5	0.805	0.901	0.894
H1-W0-0.8	63.4	0.801	0.879	0.911
H1-W0-1.1	65.2	0.812	0.882	0.920
H1-W1-0.3	56.7	0.783	0.823	0.848
H1-W1-0.6	67.0	0.808	0.994	0.812
H1-W1-0.8	75.1	0.820	0.992	0.827
H1-W1-1.1	80.3	0.842	0.988	0.852
H1-W1-1.2	81.0	0.857	0.987	0.868
H1-W1-1.3	80.5	0.860	0.974	0.884
H1-W1-1.4	81.5	0.882	0.980	0.908
H1-W2-0.6	65.3	0.770	0.960	0.802
H1-W2-0.8	77.7	0.803	1.028	0.781
H1-W2-1.1	83.3	0.775	0.994	0.780
H1-W2-1.2	84.7	0.795	1.002	0.794
H1-W2-1.3	86.1	0.816	1.016	0.803
H1-W2-1.4	86.5	0.828	1.018	0.813
H1-W3-0.6	58.6	0.697	0.882	0.791
H1-W3-0.8	71.1	0.739	0.961	0.768
H1-W3-1.0	77.8	0.741	0.982	0.755
H1-W3-1.1	79.0	0.714	0.972	0.735
H1-W3-1.2	80.1	0.717	0.982	0.730
H1-W0-0.6	73.5	0.744	0.998	0.745
H1-W0-0.8	79.7	0.764	1.005	0.760
H1-W0-1.1	82.5	0.787	1.008	0.780

Table 6 Comparison of the AISI Predictions with the Suggested Design Procedure Pedictions of ABAQUS Results (Cont.)

M_t = Ultimate moment calculated by ABAQUS (1989), k-in (1 k-in = 113 N-m)

TEST	M_t	$\frac{M_t}{M_{n\,AISI}}$	$\frac{M_t}{M_{n\,S}}$	$\frac{M_{n\,S}}{M_{n\,AISI}}$
H1-W1-0.3	73.5	0.824	1.054	0.781
H1-W1-0.6	82.8	0.803	1.082	0.742
H1-W1-0.8	92.8	0.798	1.060	0.753
H1-W1-1.1	99.8	0.819	1.074	0.763
H1-W1-1.2	101.0	0.842	1.078	0.781
H1-W1-1.3	102.0	0.857	1.071	0.801
H1-W1-1.4	101.0	0.872	1.061	0.822
H1-W2-0.6	83.9	0.794	1.054	0.753
H1-W2-0.8	99.6	0.827	1.124	0.736
H1-W2-0.9	102.0	0.823	1.118	0.736
H1-W2-0.9	104.0	0.815	1.104	0.738
H1-W2-1.0	104.0	0.798	1.078	0.740
H1-W2-1.1	106.0	0.788	1.070	0.736
H1-W3-0.6	75.5	0.716	0.945	0.758
H1-W3-0.8	93.0	0.771	1.047	0.737
H1-W3-0.9	96.4	0.755	1.031	0.732
H1-W3-1.0	97.8	0.744	1.017	0.732
H1-W3-1.1	95.1	0.685	0.955	0.718
H1-W3-1.2	103.0	0.731	1.025	0.713
Avg		0.805	0.982	
COV(%)		8.530	6.750	

Table 7 Comparison of the AISI Predictions with the Suggested Design Procedure Pedictions of Experimental Results

M_t = Ultimate moments in observed tests, k-in (1 k-in = 113 N-m)

Source	M_t	$\frac{M_t}{M_{n\,AISI}}$	$\frac{M_t}{M_{n\,S}}$	$\frac{M_{n\,S}}{M_{n\,AISI}}$
Moreyra and Pekoz (1994a)				
	127.0	0.800	0.912	0.877
	124.0	0.825	0.944	0.874
	133.0	0.904	1.045	0.865
Willis and Wallace (1990a and b)				
	86.6	0.861	0.958	0.899
	93.6	0.923	1.049	0.880
	97.0	0.998	1.071	0.932
Ellifritt and Sputo (1992)				
	144.0	0.961	1.116	0.862
	141.0	0.933	1.043	0.895
	121.0	0.903	0.901	0.891
Schuster (1992)				
	80.9	0.768	1.058	0.725
	80.9	0.768	1.058	0.725
	82.2	0.780	1.075	0.725
Avg		0.859	1.019	
COV (%)		8.940	6.640	

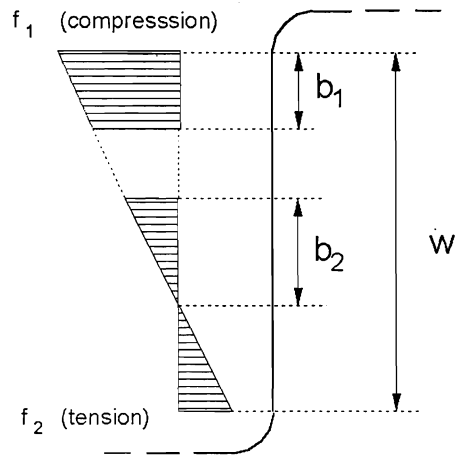

Fig. 1 Assumed effective stress area on a web as defined by the AISI Specification.

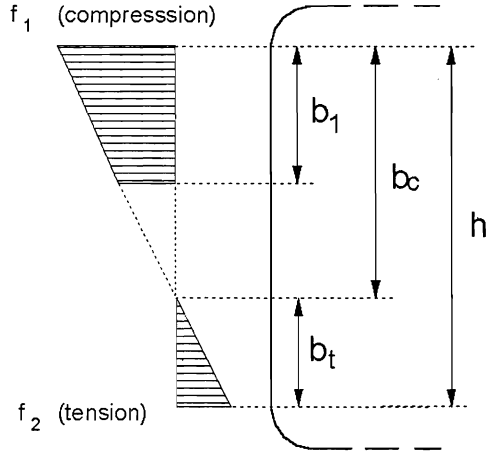

Fig. 2 Sooi's effective web model.

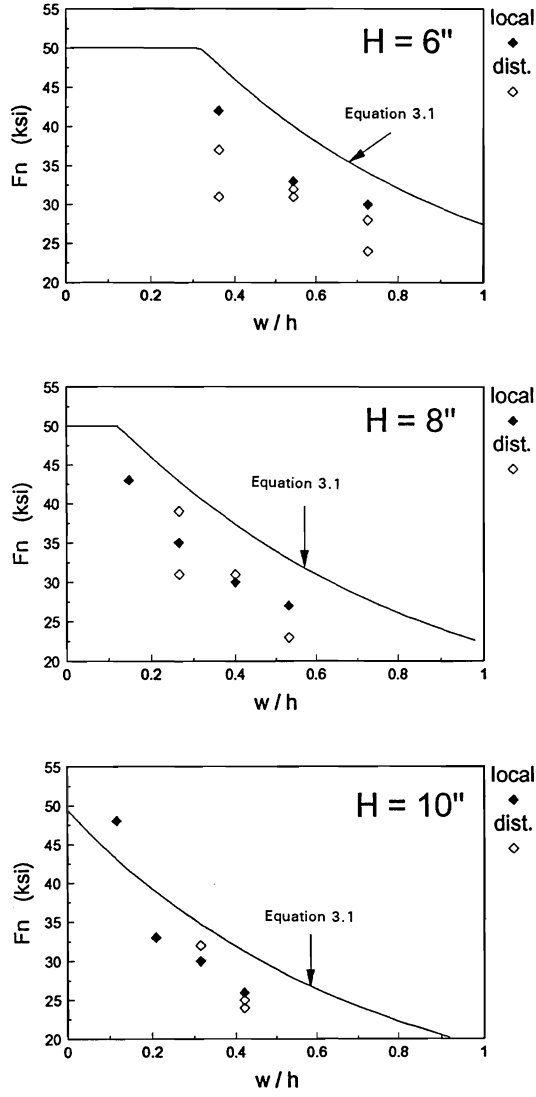

Fig. 3 Comparison of F_n (Eq. 3.1), to flange stresses determined by ABAQUS (1989)

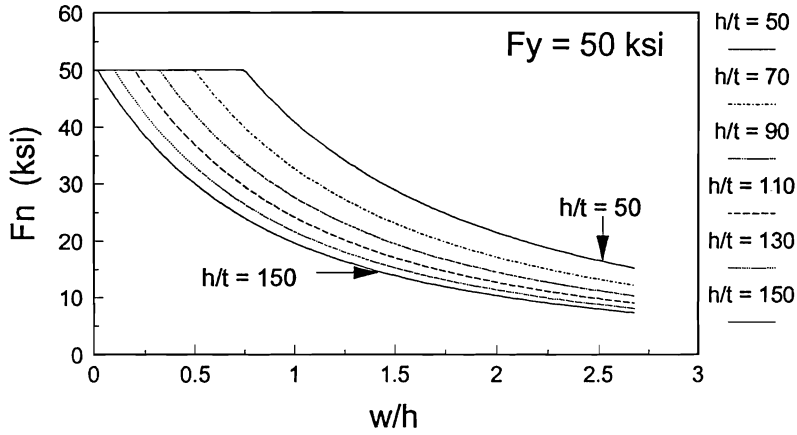

Fig. 4 The F_n function proposed by the author.

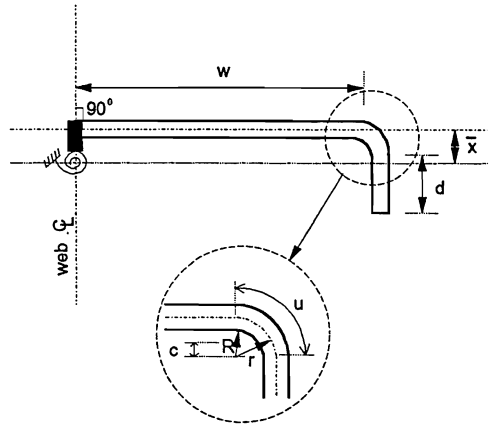

Fig. 5 Cross-section of Sharp (1966, 1993) "column" model of a lipped flange undergoing torsional buckling.